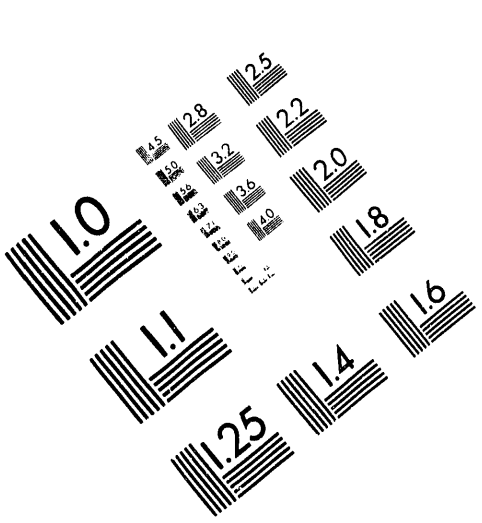

Association for Information and Image Management
1100 Wayne Avenue, Suite 1100
Silver Spring, Maryland 20910
301/587-8202

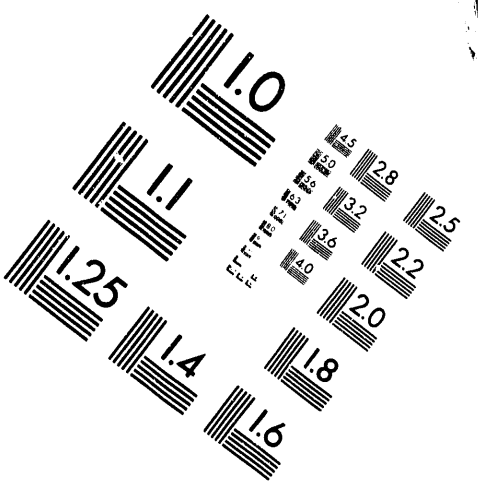

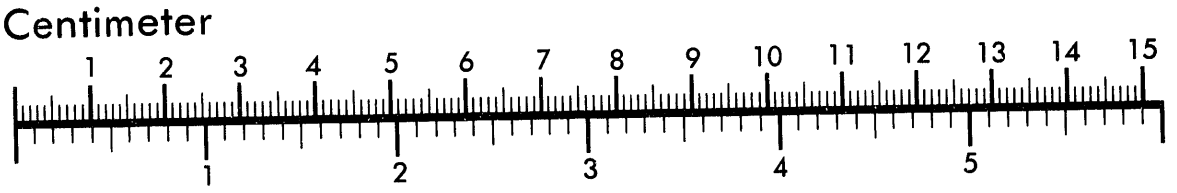

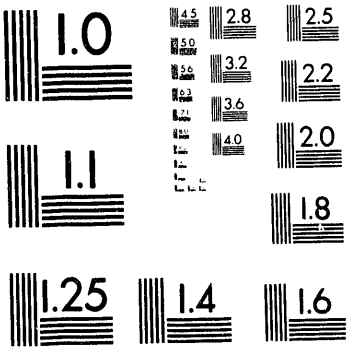

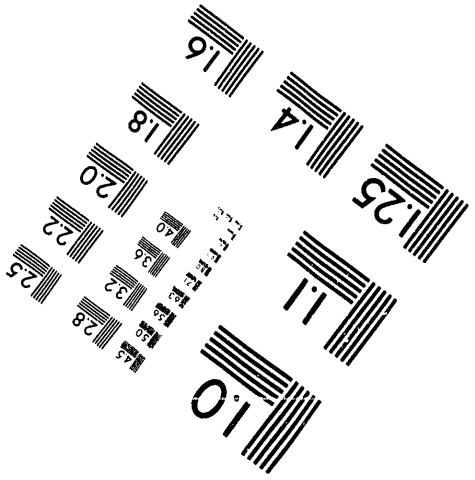

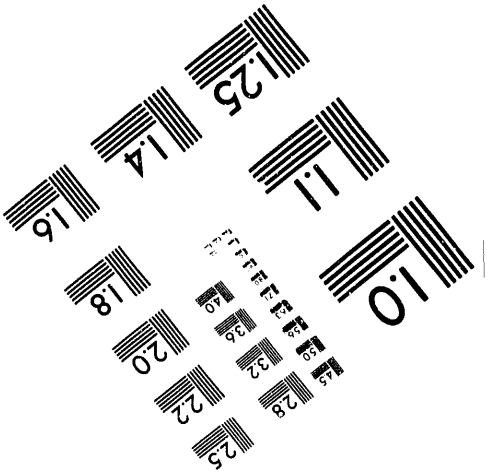

MANUFACTURED TO AIIM STANDARDS
BY APPLIED IMAGE, INC.

1 of 1

Conf-930702--35

CHAOTIC VIBRATION IN FLUIDELASTIC INSTABILITY OF A TUBE ROW IN CROSSFLOW*

S. H. Chen and S. S. Chen
Materials and Components Technology Division
Argonne National Laboratory
Argonne, Illinois 60439

* To be submitted for presentation at the 1993 ASME PVP Conference, July 25-29, 1993, Denver, Colorado

CHAOTIC VIBRATION IN FLUIDELASTIC INSTABILITY OF A TUBE ROW IN CROSSFLOW

S. H. Chen and S. S. Chen
Material and Components Technology Division
Argonne National Laboratory
Argonne, Illinois 60439

Abstract

Chaotic motions with complicated orbits make the prediction of wear between heat exchanger tubes and tube support plates difficult. To unravel the chaotic motions of nonlinearly supported tubes caused by the fluidelastic instability, an analytical investigation based on unsteady flow theory was conducted. The analytical model consists of a row of rigid tubes with three flexible tubes supported by elastic springs. This simplified model enables the study of the fluidelastic coupling effects of loosely supported tubes in crossflow.

* To be submitted for presentation at the 1993 ASME PVP Conference, July 25-29, 1993, Denver, Colorado

Nomenclature

D	Tube diameter
a_j, b_j, c_j, d_j	Clearances for Tube j
f	Vibration frequency in flow
f_v	Natural frequency of the tube in vacuum
m	Tube mass per unit length
N	Number of tubes
P	Pitch
R	Tube radius
U	Gap flow velocity in tube array
U_v	Reduced flow velocity based on frequency in vacuum (= $U/f_v D$)
u_j, v_j	Displacements of the j^{th} tube in x and y directions
x,y,z	Cartesian coordinates with x in the lift direction
α_{jk}, β_{jk}, σ_{jk} ,τ_{jk}	Added-mass coefficients
α'_{jk}, β'_{jk}, σ'_{jk}, τ'_{jk}	Fluid-damping coefficients
α''_{jk}, β''_{jk} , σ''_{jk} , τ''_{jk}	Fluid-stiffness coefficients
γ	Mass ratio (= $\rho\pi R^2/m$)
δ_s	Mass-damping ratio (= $2\,\pi\, m\zeta\,/\,\rho D^2$)
λ	Eigenvalue, also Lyapunov exponent
ω	Vibration frequency in radians
ω_v	Vibration frequency in radians in vacuum
ρ	Fluid density
ζ	Damping ratio

subscripts

j,k	Tube number (j,k = 1,N)
v	Parameters measured in vacuum

1. Introduction

Chaotic vibrations are reserved for vibrations occurring in nonlinear, deterministic systems to distinguish them from random vibrations. Since almost every physical system possesses some sort of nonlinearity, chaos happens in many places. The main feature of chaos as measured by Lyapunov exponents is sensitive dependence on initial conditions, which means that two trajectories starting close to each other in the phase space will diverge apart exponentially. Another important feature of chaos as demonstrated by bifurcation diagram is that a small change in system parameters can lead to different dynamic behaviors. For mechanical engineers, the study of chaos can help understand noisy behaviors of a system and provide better prediction of its wear or fatigue life.

An array of tubes in crossflow, commonly seen in heat exchangers, may undergo large-amplitude vibrations when the flow speed exceeds a threshold value. This phenomenon is known as fluidelastic instability and has been investigated extensively since 1970s. The motion of the unstable tubes are often limited by the support plates where clearances between the tubes and the support are usually employed to facilitate manufacturing and accommodate thermal expansion. The wear caused by the tube-support interaction is dictated by the contact forces and the angle of impact or the sliding component (Ko et al. 1984). If the tube motions are chaotic, the wear rate is hard to predict because both contact forces and the sliding speeds have no regular patterns in time.

Observations of chaos in flow-induced vibration numerically or experimentally have been reported by a number of researchers including Antunes et al. (1992), Axisa, Antunes and Villard (1988), Cai and Chen (1991 and 1992), Fricker (1992), de Langre, Hadj-Sadok and Beaufils (1992), Muntean

and Moon (1992), Paidoussis and Li (1992), and Vento, Antunes and Axisa (1992). However, all previous studies are limited to quasi-static or quasi-steady flow theory or damping-controlled instability. The objective of this paper is to investigate fluid-stiffness-controlled instability based on the unsteady flow theory incorporating all motion-dependent fluid forces.

In this paper, numerical analyses are performed on a row of rigid tubes with three tubes supported by elastic springs. Bifurcation diagrams are usually plotted first to overview the effects of a particular system parameter. Then, Poincaré maps, Lyapunov exponents, and PSDs are used to study some selected cases.

As pointed out by Baker and Gollub (1990), there are two requirements for chaos: a nonlinear element and the system is governed by at least three first-order differential equations. The tubes system discussed in this paper is capable to exhibit chaos because the system has six degrees of freedom and has a nonlinear element in the interface between tubes and the support plates. The recognition of chaos has prompted us to investigate at what specific ranges of some system parameters, the system can become chaotic. There are two ways to vary the system parameters to create chaos. The first is to increase the flow speed until two simultaneous limit cycles occur. The second is to change the configuration of tube-support system by assuming the gaps are asymmetric or the gaps on one tube are larger than those on other tubes.

2. Theory

Consider a tube row vibrating in a flow as shown in Fig. 1. The axes of the tubes are parallel to one another and perpendicular to the x-y plane. Each tube has the same radius R and the fluid is flowing with a constant flow velocity U. All tubes are assumed to be rigid, Tube 1, 2 and 3 are supported by elastic springs in the x- and y- directions, and Tube 4 and 5 are rigidly supported. The displacement components of tube j in the x- and y- direction are u_j and v_j, respectively.

Based on the unsteady-flow theory, which assumes the fluid forces are functions of tube motions, Chen (1982) has presented a general theory for the motion of tubes oscillating in fluid flow. For the j^{th} tube among a group of N tubes, the equations of motion are

$$\ddot{u}_j + 2\xi_v\omega_v\dot{u}_j + \omega_v^2 u_j + \gamma\sum_{k=1}^{N}\left(\alpha_{jk}\ddot{u}_k + \sigma_{jk}\ddot{v}_k\right) - \frac{\gamma U_v^2\omega_v^2}{\pi^3\omega}\sum_{k=1}^{N}\left(\alpha'_{jk}\dot{u}_k + \sigma'_{jk}\dot{v}_k\right) - \frac{\gamma U_v^2\omega_v^2}{\pi^3}\sum_{k=1}^{N}\left(\alpha''_{jk}u_k + \sigma''_{jk}v_k\right) = 0 \quad ,$$

and (1)

$$\ddot{v}_j + 2\zeta_v\omega_v\dot{v}_j + \omega_v^2 v_j + \gamma\sum_{k=1}^{N}\left(\tau_{jk}\ddot{u}_k + \beta_{jk}\ddot{v}_k\right) - \frac{\gamma U_v^2\omega_v^2}{\pi^3\omega}\sum_{k=1}^{N}\left(\tau'_{jk}\dot{u}_k + \beta'_{jk}\dot{v}_k\right) - \frac{\gamma U_v^2\omega_v^2}{\pi^3}\sum_{k=1}^{N}\left(\tau''_{jk}u_k + \beta''_{jk}v_k\right) = 0 \quad ,$$

where,

$$\gamma = \frac{\rho\pi R^2}{m} \quad ,$$

(2)

$$U_v = \frac{U}{f_v D} \quad ,$$

j = 1,2, and 3.

In Eqs. (1), α_{jk} , β_{jk} , σ_{jk} , and τ_{jk} are the added-mass coefficients, α'_{jk}, β'_{jk}, σ'_{jk}, and τ'_{jk} are the fluid-damping coefficients, and α''_{jk}, β''_{jk} , σ''_{jk} , and τ''_{jk} are the fluid-stiffness coefficients. The added-mass coefficients can be determined from the potential flow theory, while the fluid-damping coefficients and the fluid-stiffness coefficients have to be determined by experiments. Chen and Chandra (1991) have published these coefficients based on the experimental data by Tanaka (1980).

Equation (1) can be used to study tube vibration characteristics in flow. The study of chaos is closely related to the fluidelastic instability. Stability boundaries can be determined by setting the damping of the system equal to zero, i.e.

$$\zeta_{\text{system}} = 0 \tag{3}$$

There are some scenarios or routes through which a periodic motion (a single frequency or a small number of frequencies) becomes a chaotic motion (a broad band of frequencies). The routes to chaos which will be discussed in this paper fall into the following two categories:

Period-Doubling Route to Chaos

A periodic motion can become chaos through successive period-doublings as those demonstrated by the well-known logistic equation. A period doubling appears as a pitchfork in the bifurcation diagram. It is possible to predict the

next period-doubling because the ratio of the parameter spacings between two period-doublings is an universal number, the Feigenbaum number, 4.669 . . . .

Quasiperiodic Route to Chaos

Another common route to chaos is through quasiperiodic vibration which can be described by the following equation:

$$u(t) = A_1 \sin(\omega_1 t + \phi_1) + A_2 \sin(\omega_2 t + \phi_2) \quad (4)$$

when ω_1/ω_2 is incommensurate. It can be seen that after starting from a set of initial conditions, the above vibration (containing two vibratory components) will never return to the initial state. If the above vibration is subjected to a nonlinearity, phase-locking (subharmonic vibration) which is a precursor of chaos can occur.

3. Numerical Methods

3.1 Time Simulation Procedures

Time simulations on Eqs. (1) were performed based on the Runge-Kutta method. The time increment, dt, is chosen as 0.0001 second which will divide each cycle into about 500 time steps. Since only the final states are interested, the initial conditions were chosen as $u_1 = u_2 = u_3 = v_1 = v_2 = v_3 = 0.99$ of the gap size and all $du_j/dt = 0$ in order to reduce the transient time and to make sure that all possible vibration modes are excited. Note that the choice of initial conditions

can sometimes determine which basin of attraction the motion is going to fall into, but other than this, initial conditions have no effects on limit cycle vibrations.

The data of the first 100 cycles of simulation are always discarded. For producing PSDs and Lyapunov exponents, about 100 cycles of the time series data are needed; for bifurcation diagrams, about 60 cycles are needed for each case; and for Poincaré maps, about 1000 cycles are needed.

3.2 Tools for Identifying Chaos

Bifurcation Diagram

The change in the number of solution of a differential equation system as a parameter varied is called a bifurcation. It is called the Hopf bifurcation when the system changes from a stable state to a limit cycle. The bifurcation diagrams are produced by slowly varying a system parameter and plotting the velocity of Tube 2 in the x-direction whenever Tube 1 moves from -x to +x. Bifurcation diagrams provide an overview of a system, but the results have to be checked by other mathematic tools. For example, the quasiperiodic and the chaotic motions cannot be distinguished in the bifurcation diagram.

Poincaré Map

The Poincaré map is a powerful technique for identifying chaotic motions. The map consists of strobed pictures of the phase space. Periodic motion will appear as a point in the Poincaré map, subharmonic will be a finite number of

points, quasiperiodic will be a closed curve, and chaos will be a cloud of unorganized points.

For a forced vibration, the strobing frequency is usually chosen as the forcing frequency. Since there is no forcing frequency in the current system, the displacement in the x-direction of Tube 1 is used as the triggering signal. The displacements and velocities of Tube 2 are recorded whenever Tube 1 move from -x to +x. This is actually the same method used in sampling the data for the bifurcation diagram.

Power Spectral Density (PSD)

For a periodic motion, discrete frequencies dominate in the power spectrum, while chaos has a broad-banded spectrum, though some peaks may still be discernable. PSDs are produced by Fourier transforms on time series data. The appearance of subharmonic frequency in the PSD is the precursor of chaos through the quasiperiodic route.

Lyapunov Exponents

Lyapunov exponents provide a means to quantitatively measure the chaos, while the other methods mentioned above only predict whether a vibration is chaotic or not. Lyapunov exponents are defined as the average exponential rates of divergence or convergence of nearby orbits in phase space, and they can be calculated by

$$\lambda = \frac{1}{t_n - t_0} \sum_{k=1}^{N} log_2 \frac{d(t_k)}{d_0(t_{k-1})} \tag{5}$$

where λ is a Lyapunov exponent, $d_0(t_{k-1})$ is the initial distance between the two starting points, and $d(t_k)$ is the final distance after a time step. If the motion is periodic, the exponents are negative or zero, and if the motion is chaotic, the exponents are positive. A more detailed review on Lyapunov exponents has been presented by Wolf et al. (1985).

4. Results and Discussion

4.1 System Configuration

The system consists of a row of rigid tubes with three tubes flexibly supported by elastic springs as shown in Fig. 1. The degree of freedom of the system is six - three flexibly supported tubes each has two degrees of freedom (in the x- and y- directions). There are many parameters involved in the tube-support plate system, thus, it is necessary to chose a small number of parameters as variables and fix the rest of parameters.

Variable parameters:

Reduced flow velocity, U_V

Mass-damping parameter, δ_S (set at 25 for dynamic analyses)

Tube-support plate gaps, a_j, b_j, c_j, and d_j (The openings on the

support plate are assumed to be squares as shown in Fig. 2).

Constant parameters:

The tube diameter and the pitch/diameter ratio:

$D = 0.0254$ m

$P/D = 1.33$

The natural frequency of the tube:

$f_v = 20$ Hz before contact

$f_v = 250$ Hz after contact

The structural damping of the tube:

$\zeta_v = 0.02$

4.2 Steady State Solutions

The fluidelastic stability boundaries, on which the system damping equal to zero, can be calculated using procedures presented by Chen (1983 and 1989). For a range of U_v and d_s, the boundaries are plotted in Fig. 3. The two unstable regions correspond to the fluid-damping-controlled instability and the fluid-stiffness-controlled-instability regions, respectively. The stability curve for a single flexible tube in a rigid tube row is also plotted with a dotted curve. For a single flexible tube, the instability is caused by the fluid-damping-controlled instability mechanism.

For later dynamic analyses, δ_S will be fixed at 25. The real parts of the six eigenvalues of the system as functions of U_V for $\delta_S = 25$ are plotted in Fig. 4. Any mode with a positive real part is unstable. The first critical value of U_V is 67 when Mode 1 become unstable (first Hopf bifurcation). The second critical value of U_V is 114 when Mode 2 become unstable (second Hopf bifurcation). The instability modes are also given in Fig. 4. The other four modes(dotted lines) are always stable. Note that these two critical values, 67 and 114, are obtained from the steady state solutions using the linear theory without support plate.

4.3 Motions of Two Simultaneous Limit Cycles (all Gaps equal to 0.1 D)

When U_V is between the first and the second critical values, the tube motions are periodic if all gaps are of the same size. If U_V is above the second critical value, then there exists two simultaneous limit cycles and the motions may become chaotic. This section investigates this type of chaos.

Tube Orbits and Phase Plane Portraits

The most direct information about the tube motion comes from the tube orbits and the phase planes (Figs. 5). When $U_V = 122$, both Mode 1 and Mode 2 are unstable, and the motions are apparently dominated by the these two modes. First, the beat phenomenon caused by the interaction of these two modes is noticed. At the particular moment shown in Fig. 5a, the amplitude of Tube 3 is almost zero because Mode 1 and Mode 2 cancel each other out, while Tube 2 is at its maximum amplitude which is the sum of the two modes. Furthermore, two basins of attraction appear in the phase plane of Tube 1.

Bifurcation Diagram

Figure 6 shows the bifurcation diagram, in which U_V is slowly increased to observe the change of dynamic behavior. The y axis is the velocity of Tube 2 whenever Tube 1 moves from -x to +x. In this figure, at least four periodic windows are visible. These windows are caused by "phase-locking" which is the precursor of chaos. The largest window, from U_V = 118 to U_V = 119.5, is enlarged and shown in Fig. 6b. In the bifurcation diagrams, both quasiperiodic motion and chaotic motion show the same type of scattered pattern (infinite number of points), thus, it is necessary to use Poincaré maps to distinguish them.

Poincaré Maps, PSDs, and Lyapunov Exponents (Fig. 7)

According to the bifurcation diagram, three specific U_V values are selected for more detailed investigations. First, when U_V = 110, the motion is quasiperiodic. The Poincaré map is a closed curve. In the PSD, two peaks corresponding to two incommensurate frequencies are discernible. The higher harmonic components (three times of the dominant frequency) are caused by the contacts between the tubes and the support plates. The PSDs here are for the vibrations of Tubes 1 and 2 in the x-direction. The Lyapunov exponent is positive.

Second, when U_V = 118.7 the motion is subharmonic due to phase-locking. The Poincaré map contains a finite number of points. In PSD, subharmonic frequencies, especially the one of 2 Hz, appear. It is interesting to note that the Lyapunov exponent is negative. This means that Lyapunov exponents are

capable to distinguish between the quasiperiodic vibration (positive for U_V = 110) and the subharmonic vibration (negative for U_V = 118.7).

Third, when U_V = 122, the motion is chaotic. The Poincaré map is a broken curve with a fractal structure. In PSD, the frequency spectrum is very noisy. Without any surprise, the Lyapunov exponent is positive.

Contact Forces and Wear between Tubes and the Support Plates

Contacts between tubes and the support plate are the culprit of chaos. The time history of contact forces, shown in Fig. 8a, can be used to explain why the motion is quasiperiodic or chaotic. For U_V = 118.7, the contacts forces seem to follow a periodic pattern, thus, the motions are subharmonic. Wear between tubes and the supports plates, which is dependent on the contact forces and the sliding speed, is very difficult to predict if the motions are chaotic. This can be seen from Fig. 8b, where the time histories of wear rates for U_V =122 (chaotic) are plotted.

4.4 Effects of the Configuration of Tube-Support System on Tube Motions

To demonstrate that it does not necessarily need two simultaneous limit cycles to create chaos, two values of U_V, 80 and 100 (below the second critical value of 114), are selected for further study. Here, instead of varying U_V, the geometry of the openings is varied. There are two ways of varying the configuration of the tube-support system. This first is to assume the gap is asymmetric and vary the size of one gap while keep the rest of gaps as constants.

The second is to assume that $(gap)_1 \neq (gap)_{2,3}$ and vary the ratio of $(gap)_1$ and $(gap)_{2,3}$ with $(gap)_{2,3} = 0.1$ D. Here, $(gap)_j$ represents the gap size of Tube j.

Effects of Asymmetric Gap on Tube Motions - All a_j, b_j, c_j and $d_j = 0.1$ D, Except a_1 is a Variable

It is common that the equilibrium positions of the tubes are not at the center of the openings. In the bifurcation diagrams, Figs. 9, the control parameter is a_1 which is slowly varied while the rest of gaps remain at 0.1 D. It can be found that either when $U_V = 80$ or $U_V = 100$, if the gap is almost symmetric, the motion is periodic with only one frequency. If a_1 is decreased, the motion first bifurcates to a period-2 vibration and then to a period-4 vibration. However, no further bifurcation after the period-4 bifurcation. This is because when $a_1 < 0.098$ (for $U_V = 80$) or $a_1 < 0.094$ (for $U_V = 100$), the contacts have become one-sided (known from the time series data not included in this paper). Also, in the bifurcation diagrams, the y-axis is du_1/dt instead of the usual du_2/dt, this is simply because that using du_1/dt happens to produce better bifurcation diagrams.

A Poincaré map along with its PSD are plotted in Figs. 10 for $U_V = 80$ with $a_1 = 0.096$. The motion is a period-4 subharmonic oscillation.

Effects of the Ratio of $(gap)_1$ and $(gap)_{2,3}$ on Tube Motions

It is possible that not all the openings on the support plates are of the same size. In the bifurcation diagrams, Figs. 11, the control parameter is the ratio of $(gap)_1$ and $(gap)_{2,3}$ which is slowly varied. It can be seen that for $U_V =$

80, except when the ratio is between 3 and 3.6 and between 2 and 2.2, the motions are periodic. When U_V =100, the two areas have multiple solutions are from 3.1 to 3.7 and from 1.6 to 2.7.

A Poincaré map along with its PSD are plotted in Figs. 12 for U_V = 100 with $(gap)_1/(gap)_{2,3}$ = 3.34. The chaotic motion is very pronounced for this case.

Note that this paper only discusses square openings while the real openings may be circular and there also is friction between the tubes and the supports. However, some calculations have been performed for circular openings; it is found that the circular openings and friction have no significant effect on the bifurcation phenomenon.

5. Closing Remarks

An analysis using time simulations, PSDs, bifurcation diagrams, Poincaré maps, and Lyapunov exponents is performed to investigate the motions of a row of loosely supported tubes in crossflow. This is the first study on the chaotic vibration associated with stiffness-controlled instability of loosely supported tubes on the basis of the unsteady flow theory.

For a range of system parameters, the flow-induced instability is periodic with a single frequency. The periodic motion can become chaotic through the following ways: (1) U_V is increased until the second Hopf bifurcation occurs; (2) the gap is asymmetric; (3) the gaps for one tube are larger than those of other tubes.

The route to chaos through quasiperiodic vibration has been demonstrated by the two simultaneous limit cycle case. It is shown that the precursor of this type of chaos is the subharmonic oscillation caused by phase-locking.

Contacts between the tubes and the support plate are the culprit of the chaos. The time history of contact forces can somewhat explains why the motions are quasiperiodic or chaotic. It is also found that due to chaotic motions, wear rates can become very difficult to predict.

This paper demonstrates how chaos occurs, but the practical uses of chaos is relatively untapped. Three particular questions along this line of thought are: (1) How significant is the effects of chaos on the wear or fatigue life? (2) How useful is the recognition of chaos in identifying the sources of the peaks in the frequency spectrum of a system? (3) Is it practical to use the bifurcation feature to monitoring the changes of parameters in mechanical systems?

Acknowledgments

This work was sponsored by the U.S. Department of Energy, Office of Basic Energy Science, Division of Engineering and Geosciences, under Contract W-31-109-Eng-38.

The authors wish to express their gratitude to Dr. Y. Cai for his assistance in the numerical methods for identifying chaos.

References

Antunes, J., de Langre, E., Vento, M. A., and Axisa, F. 1992, "A Theoretical Model for the Vibro-Impact Motions of Tubes Bundles Under Fluidelastic Instability," presented at the ASME Winter Annual Meeting, Nov. 9-13, 1992, Anaheim, CA.

Axisa, F., Antunes, J., and Villard, B., 1988, "Overview of Numerical Methods for Predicting Flow-Induced Vibration," Trans. of ASME, J. of Pressure Vessel Technology, Vol. 110, pp 6-14.

Baker, G. L., and Gollub, J. P., 1990, Chaotic Dynamics an Introduction, Cambridge University Press.

Cai, Y., and Chen, S. S., 1991, "Chaotic Dynamics of Loosely Supported Tubes in Crossflow," Argonne National Laboratory Report ANL-91/30.

Cai, Y., and Chen, S. S., 1992, "Chaotic Vibrations of Nonlinearly Supported Tubes in Crossflow," presented at the ASME Winter Annual Meeting, Nov. 9-13, 1992, Anaheim, CA.

Chen, S. S., and Jendrzejczyk, J. A., 1982, "Stability of Tube Arrays in Crossflow," Nuclear Engineering and Design Vol. 75, pp 351-374.

Chen, S. S., 1983, "Instability Mechanisms and Stability Criteria of a Group of Circular Cylinders Subjected to Cross-Flow. Part 1: Theory; Part 2: Numerical Results and Discussions." Trans. of ASME, J. of Vibration, Acoustics, Stress, and Reliability in Design, Vol. 105, pp 51-58 and 253-260.

Chen, S. S., 1989, "Some Issues Concerning Fluid-Elastic Instability of a Group of Circular Cylinders in Cross-Flow," Trans. of ASME, J. of Pressure Vessel Technology, Vol. 111, pp 507-518.

Chen, S. S., and Chandra, S., 1991, "Fluidelastic Instabilities in Tube Bundles Exposed to Nonuniform Cross-Flow," Journal of Fluids and Structures 5, pp 299-322.

Fricker, A. J., 1992, "Numerical Analysis of the Fluidelastic Vibration of a Steam Generator Tube with Loose Supports," Journal of Fluids and Structures, Vol. 6, pp 85-107.

de Langre, E., Hadj-Sadok, C., and Beaufils, B., 1992, "Non-Linear Vibrations Induced by Fluidelastic Forces in Tube Bundles," presented at the ASME Winter Annual Meeting, Nov. 9-13, 1992, Anaheim, CA.

Ko, P. L., and Basista, H., 1984, "Correlation of Support Impact Force and Fretting-Wear for a Heat Exchanger Tube," Trans. of ASME, J. of Pressure Vessel Technology, Vol. 106, pp 69-77.

Muntean, G. C., and Moon, F. C., 1992, "Multifractals in Flow-Induced Vibrations," Proceedings of the Tenth Symposium on Energy Engineering Sciences at Argonne National Laboratory, pp 226-232.

Paidoussis, M. P., and Li, G. X., 1992, "Cross-Flow-Induced Chaotic Vibrations of Heat-Exchanger Tubes Impacting on Loose Supports," Journal of Sound and Vibration, Vol. 152(2), pp 305-326.

Tanaka, M., 1980, "Study on Fluidelastic Vibrations of Tube Bundle," Japan Society Mechanical Engineering, Trans., Section B, Vol. 46(408), pp 1398-1407.

Vento, M. A., Antunes, J., and Axisa, F. 1992, "Tube/support Interaction under Simulated Fluidelastic Instability: Two-Dimensional Experiments and Computations of the Nonlinear Response of a Straight Tube," presented at the ASME Winter Annual Meeting, Nov. 9-13, 1992, Anaheim, CA.

Wolf, A., Swift, H. B., Swinney, H. L., and Vastano, J.A., 1985, "Determining Lyapunov Exponents from a Time Series," Physics, Vol. 16D, pp 285-317.

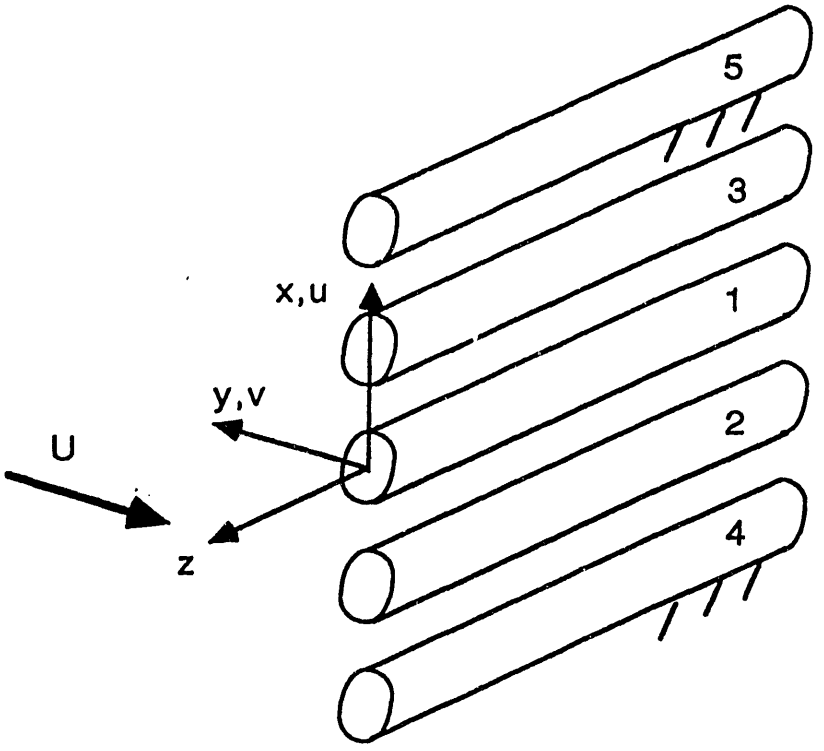

Figure 1. The configuration of the tube system.

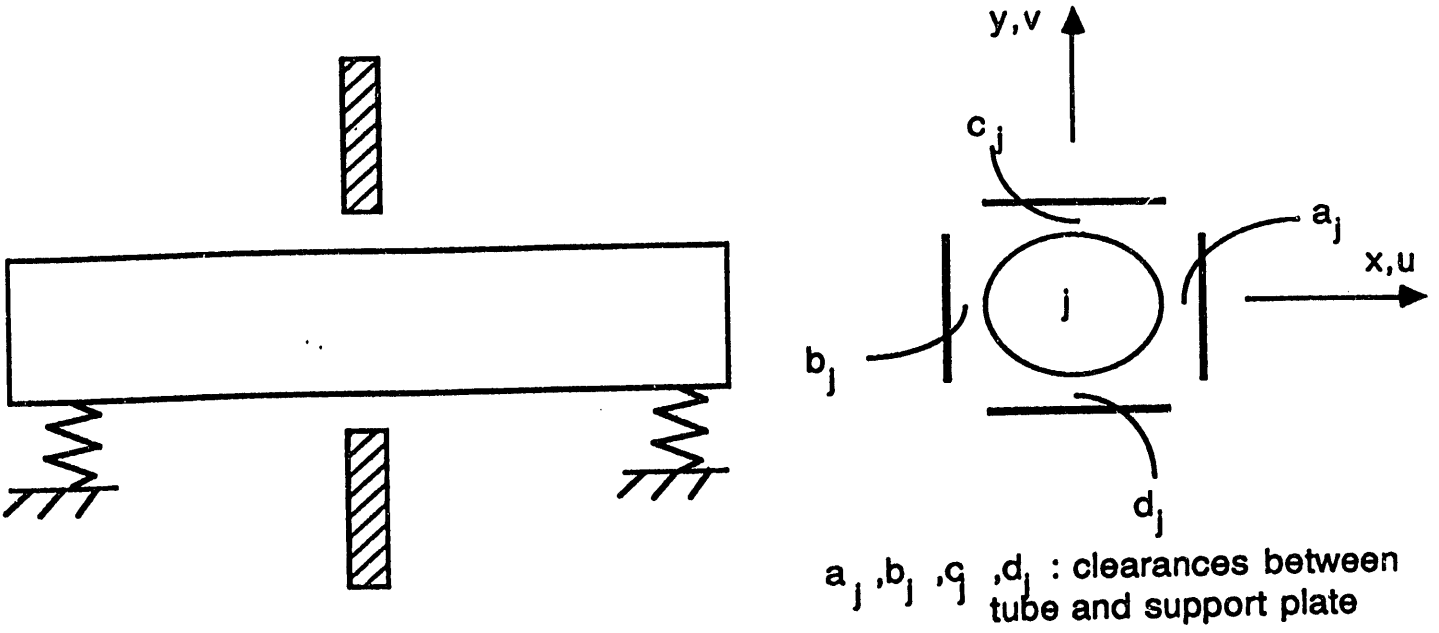

Figure 2. Rigid tubes supported by elastic springs and gaps between tubes and the support plates.

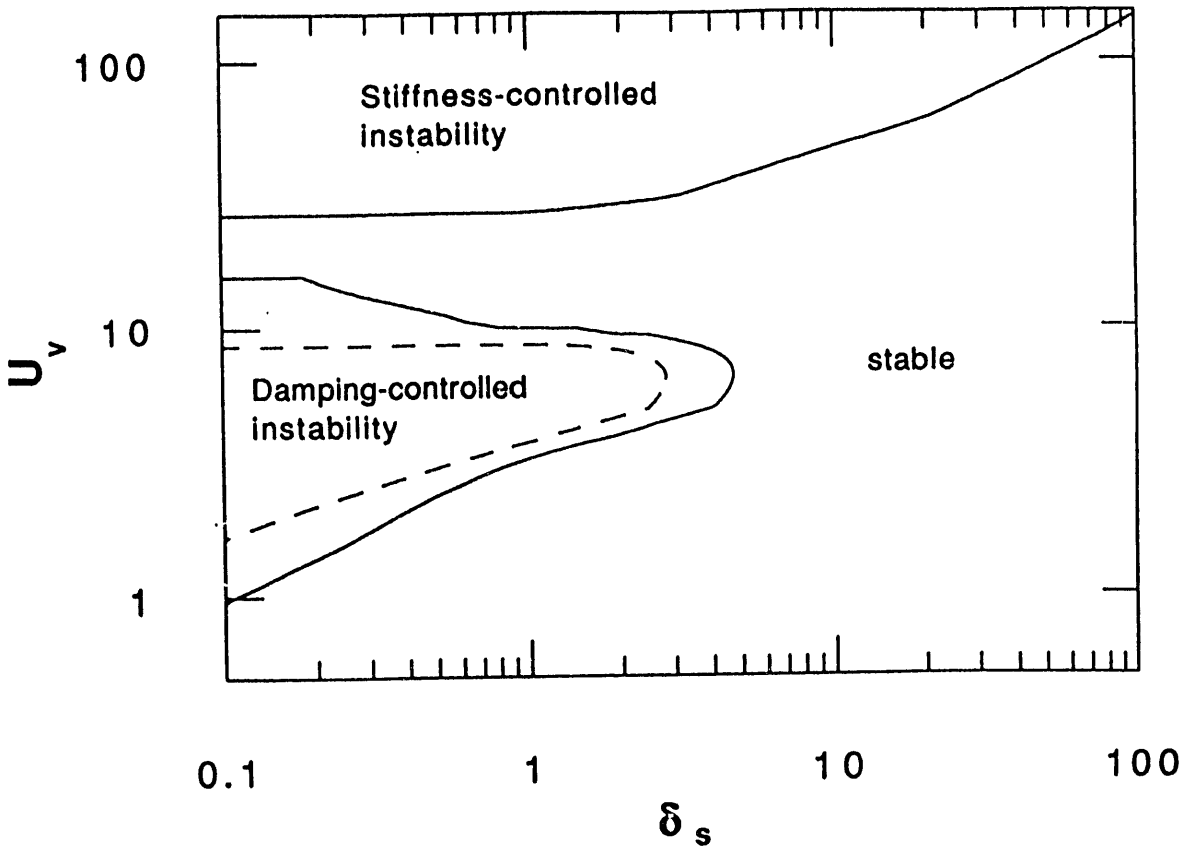

Figure 3. The stability boundaries of a row of five tubes (the dotted curve is for a elastic tube in a rigid tube row).

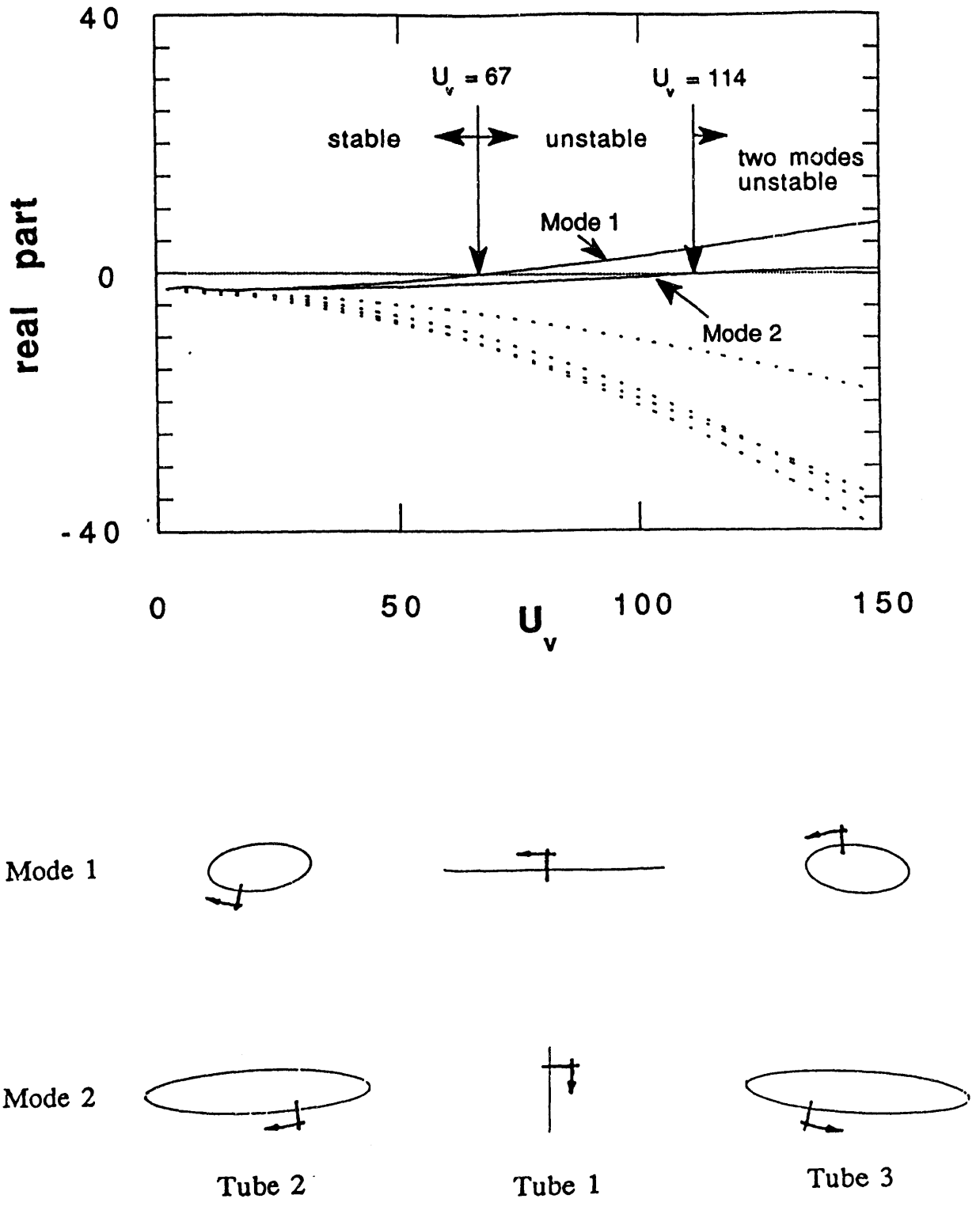

Figure 4. The real parts of the eigenvalues for Eqs. (1) when $\delta_s = 25$.

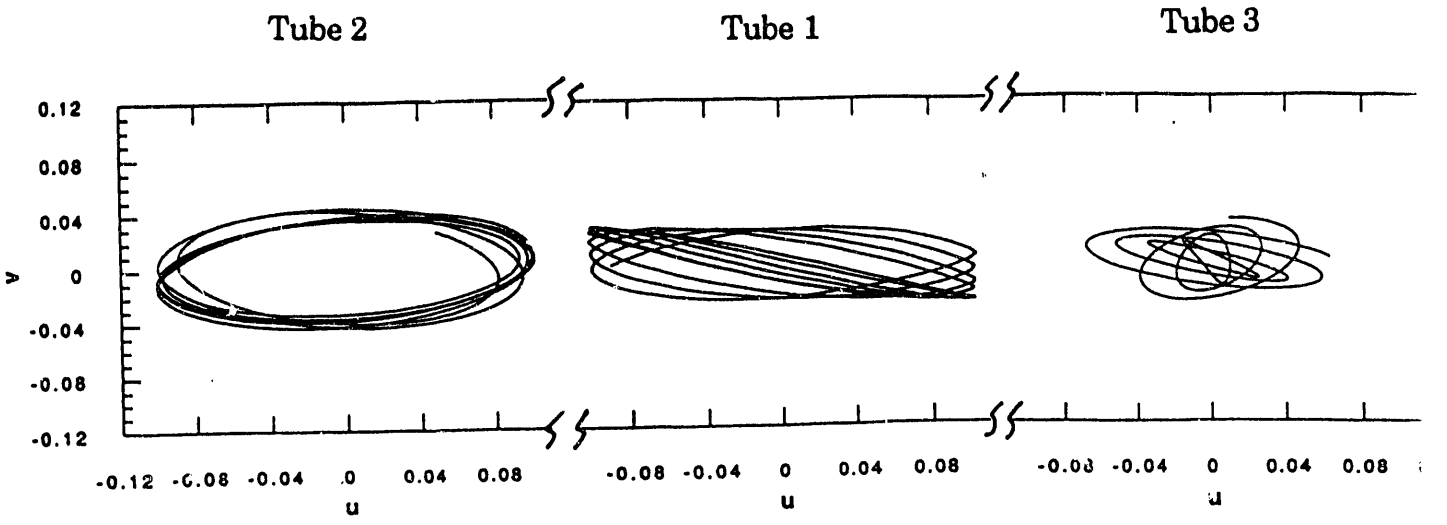

(a)

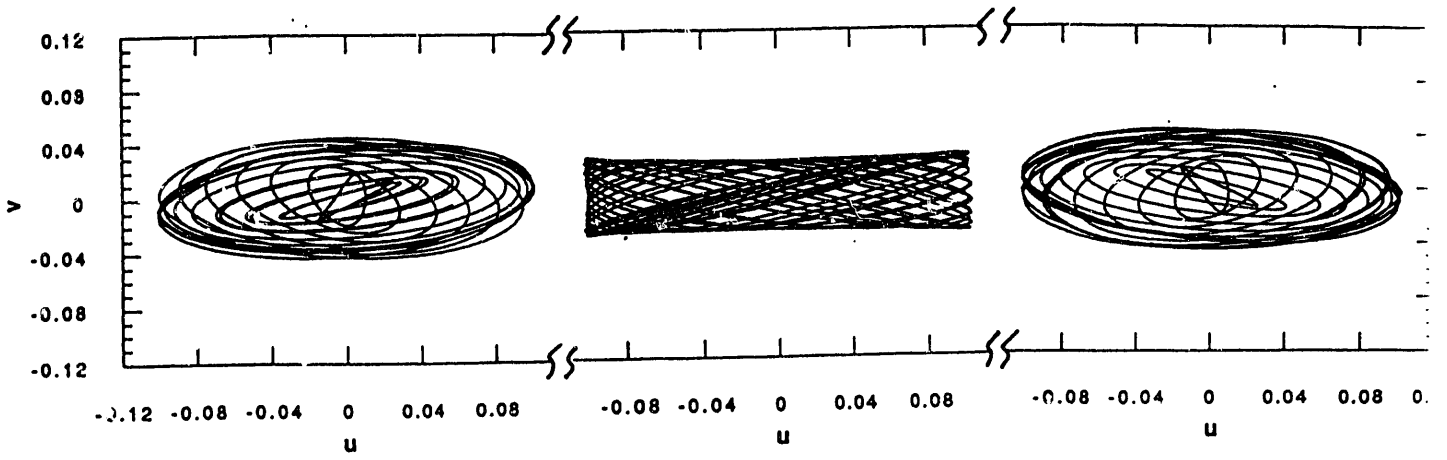

(b)

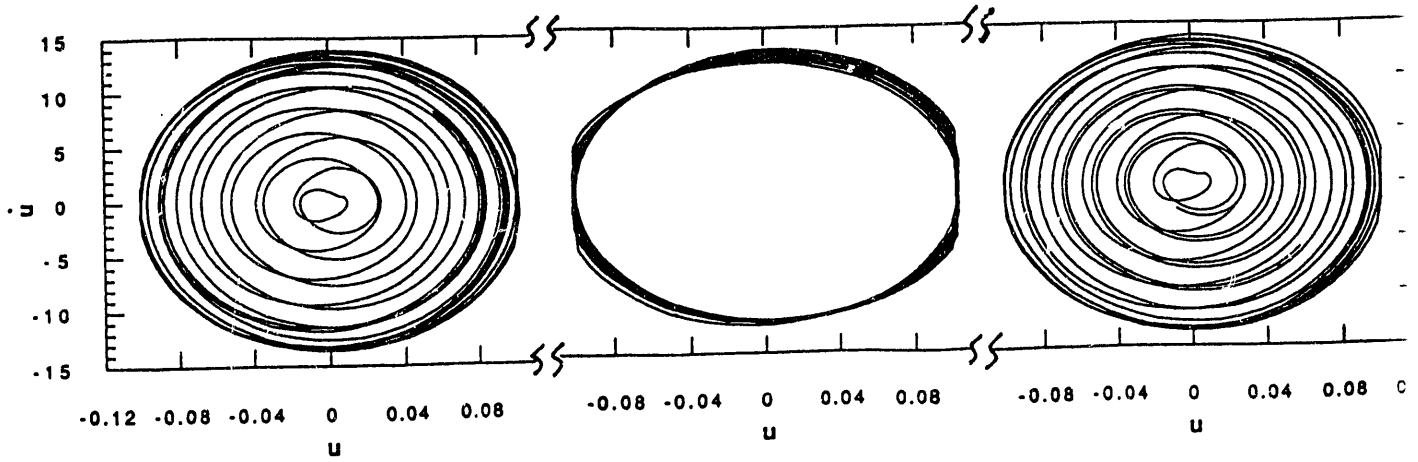

(c)

Figure 5. Tube orbits and phase planes for $U_v = 122$ and $\delta_s = 25$ (chaotic motion): (a) 6 orbits (b) 18 orbits (c) phase planes for the x-

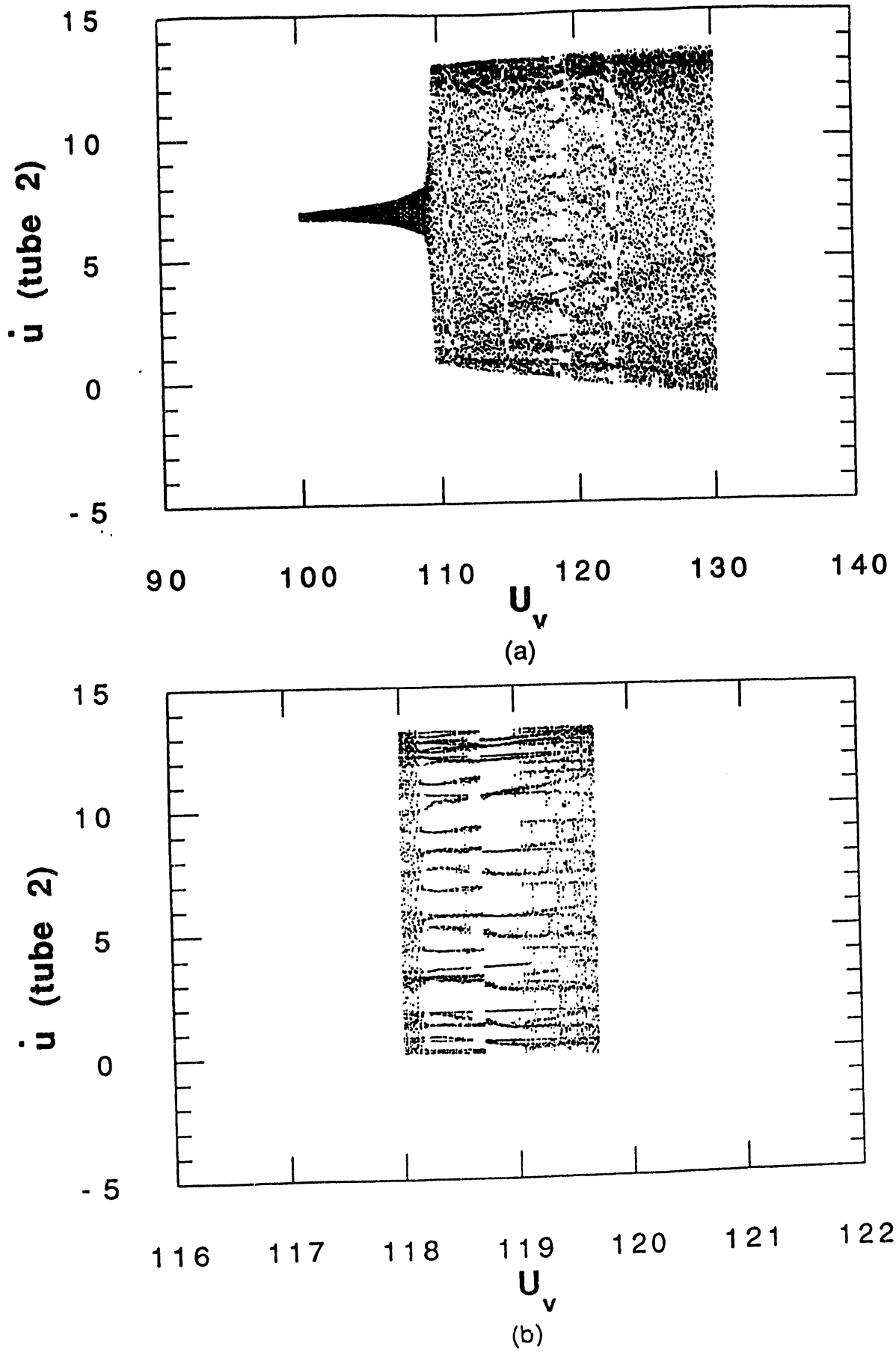

Figure 6. Bifurcation diagram for two simultaneous limit cycles (occur when U_v > second critical speed).

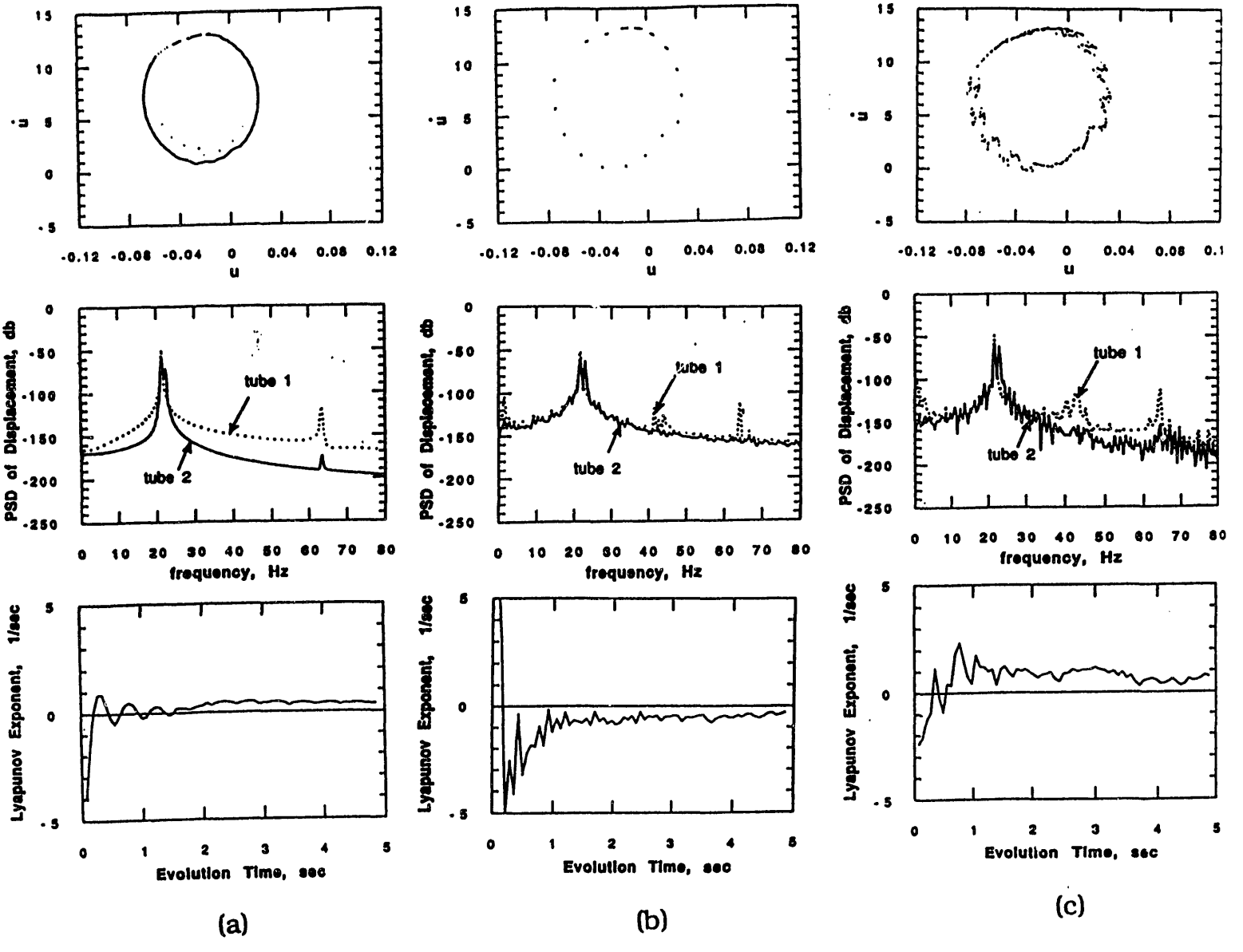

Figure 7. The Poincare Maps, PSDs, and Lyapunov exponents for (a) U_V = 110 (quasiperiodic), (b) U_V = 118.7 (phase–locking, subharmonic), and (c) U_V = 122 (chaotic).

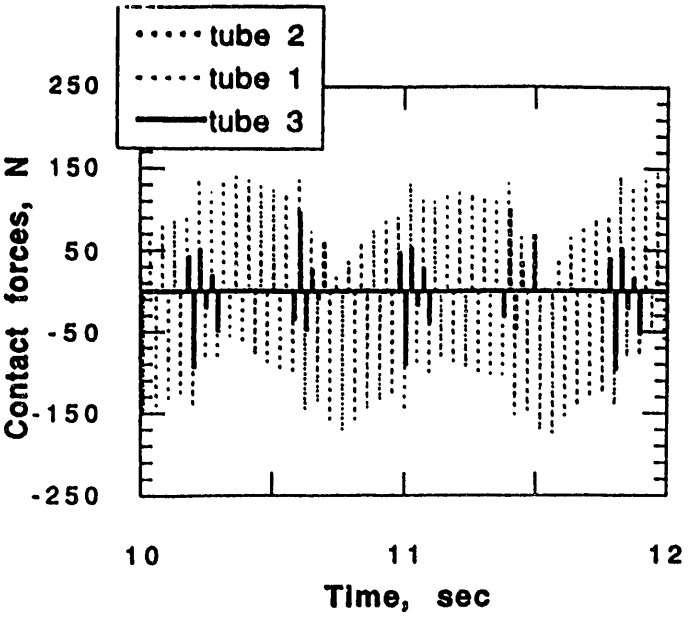

(a)

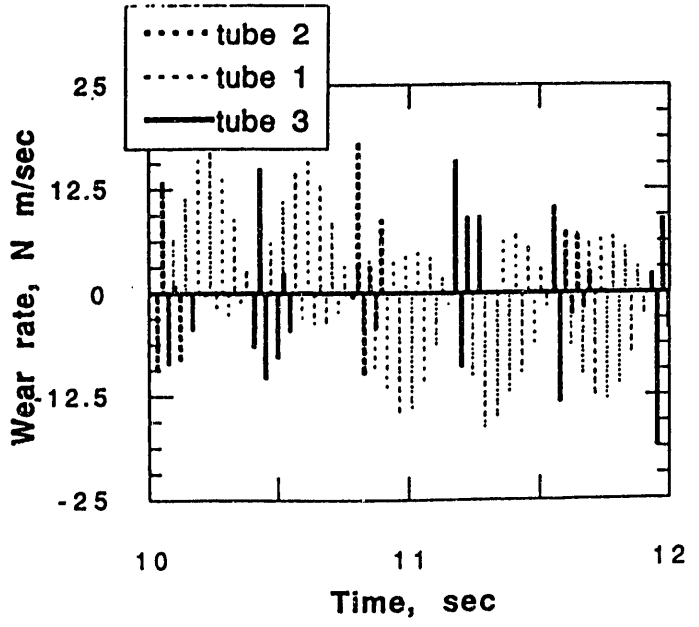

(b)

Figure 8. (a) Time histories of contact forces for U_v = 118.7 (subharmonic), periodic pattern can be seen. (b) Time histories of wear rates (contact forces time sliding speeds for U_v = 122 (chaotic), no periodic pattern. The sign indicates which side of a tube is in contact.

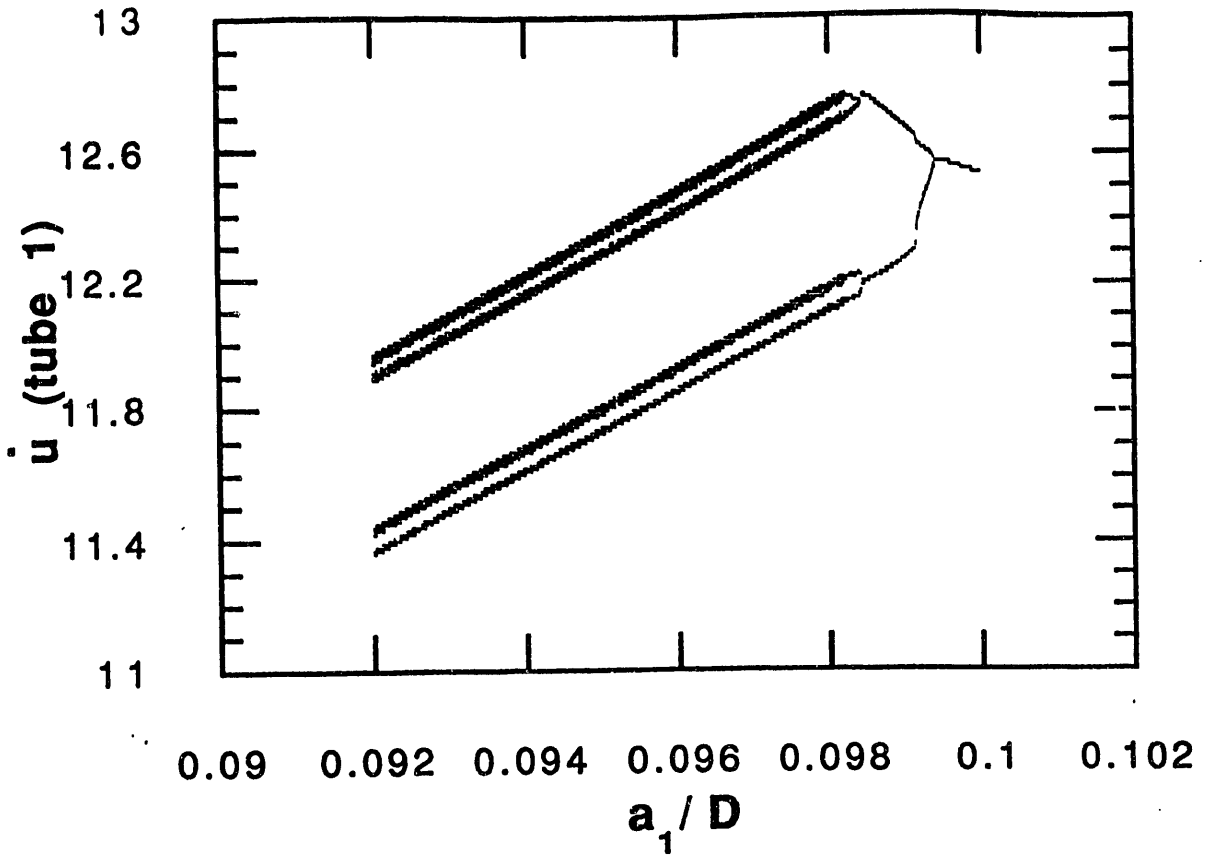

(a)

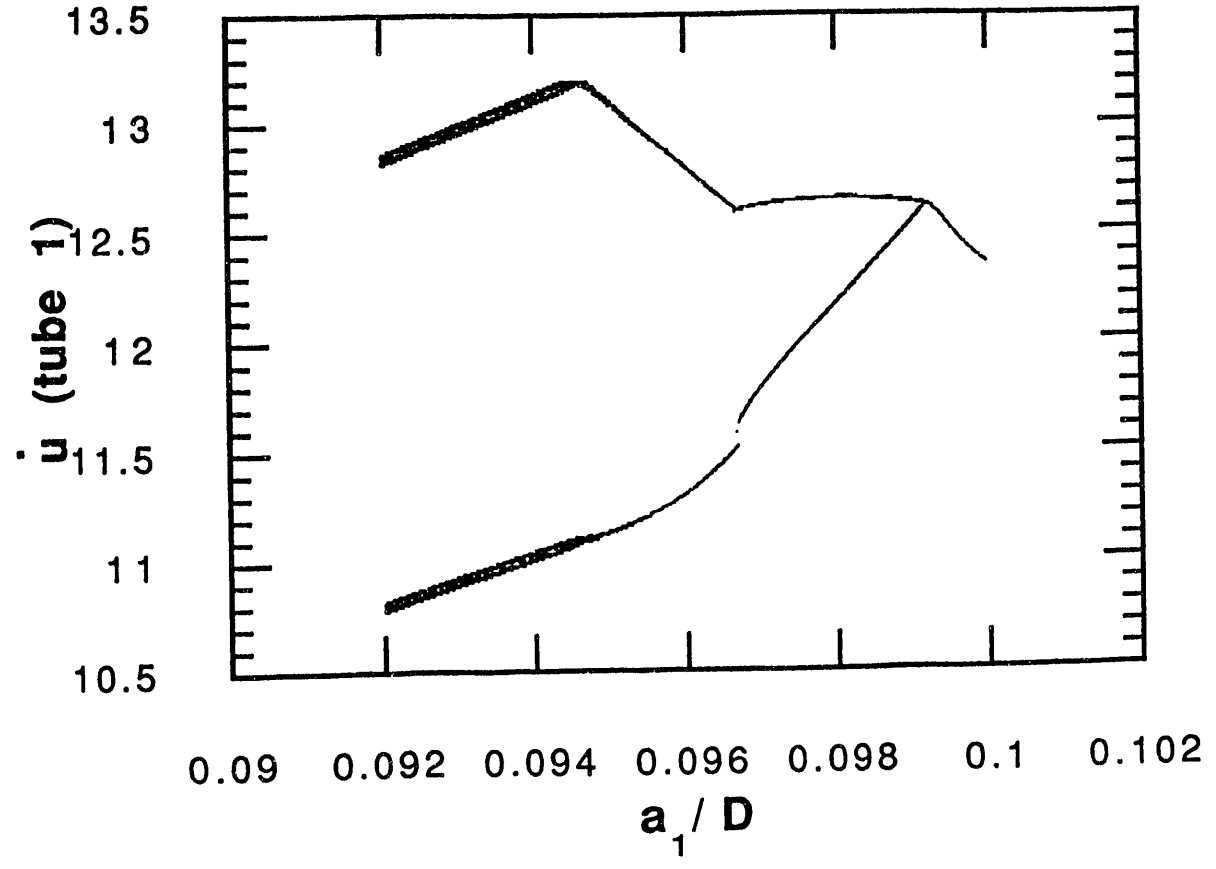

(b)

Figure 9. Bifurcation diagrams for asymmetric gaps. All a_j, b_j, c_j, d_j = 0.1 D, except a_1 is a variable. (a) U_v = 80 (b) U_v = 100.

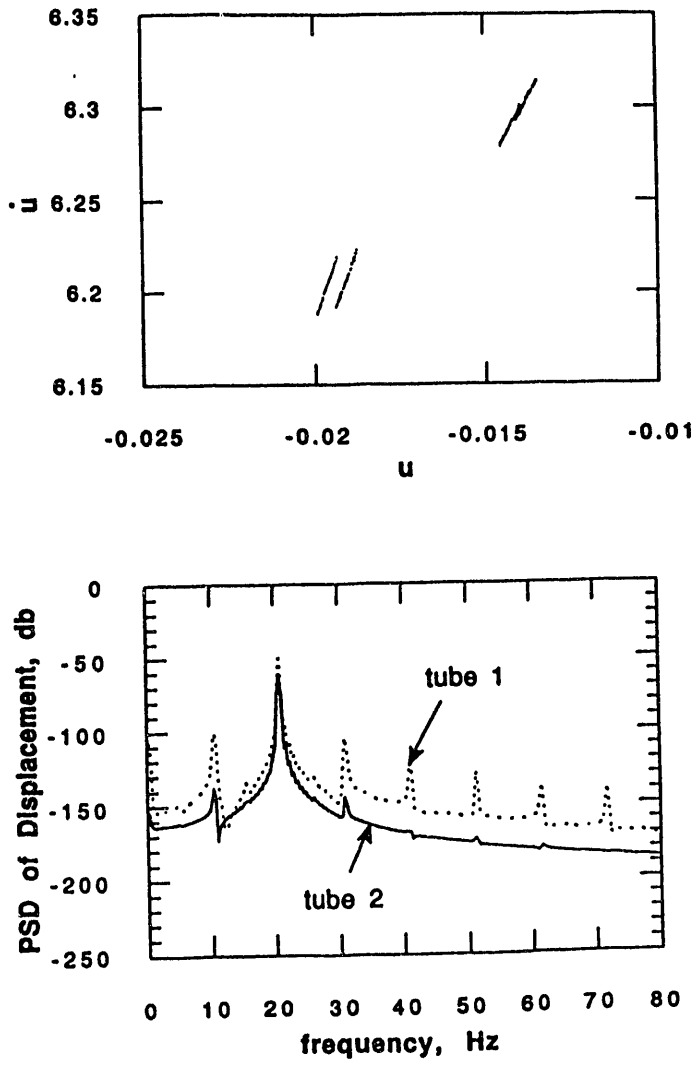

Figure 10. Poincare map & PSD for asymmetric gaps: $U_v = 80$, $a_1 = 0.096$ (period–4 motion).

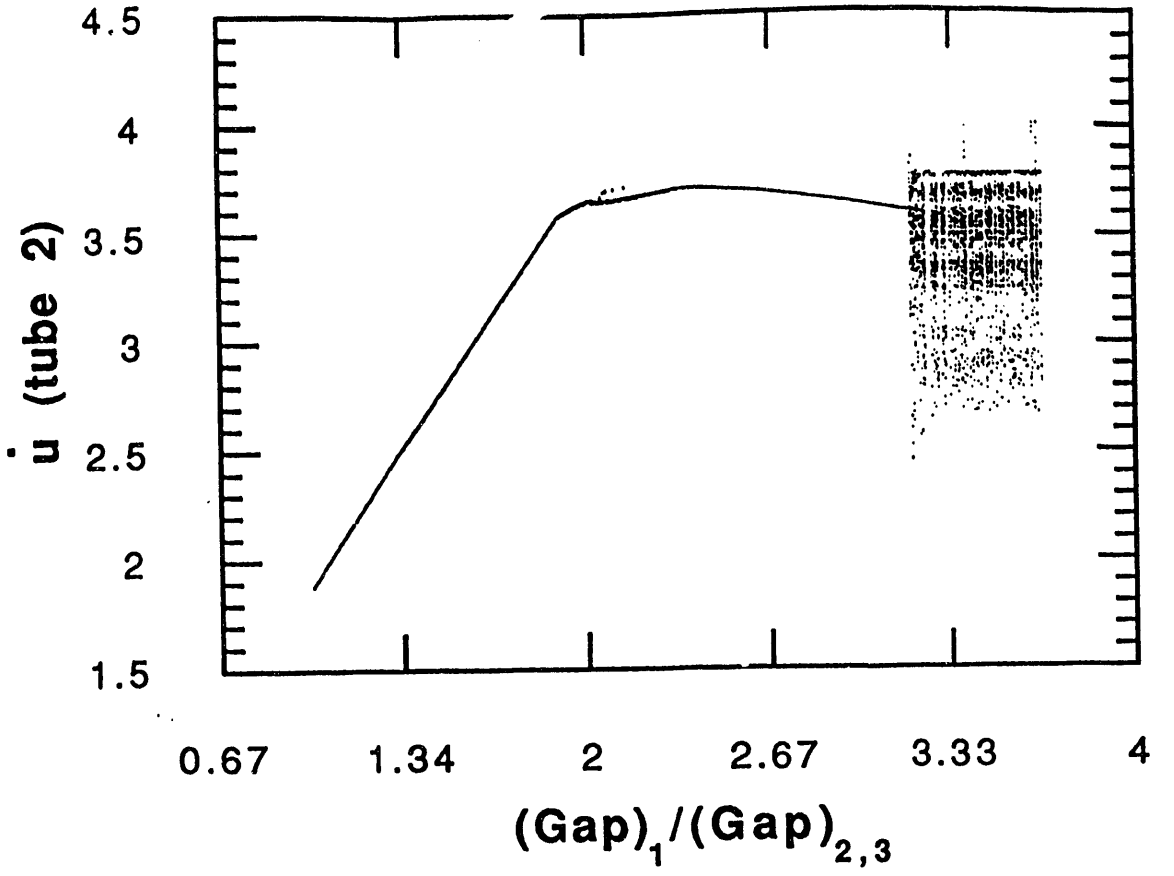

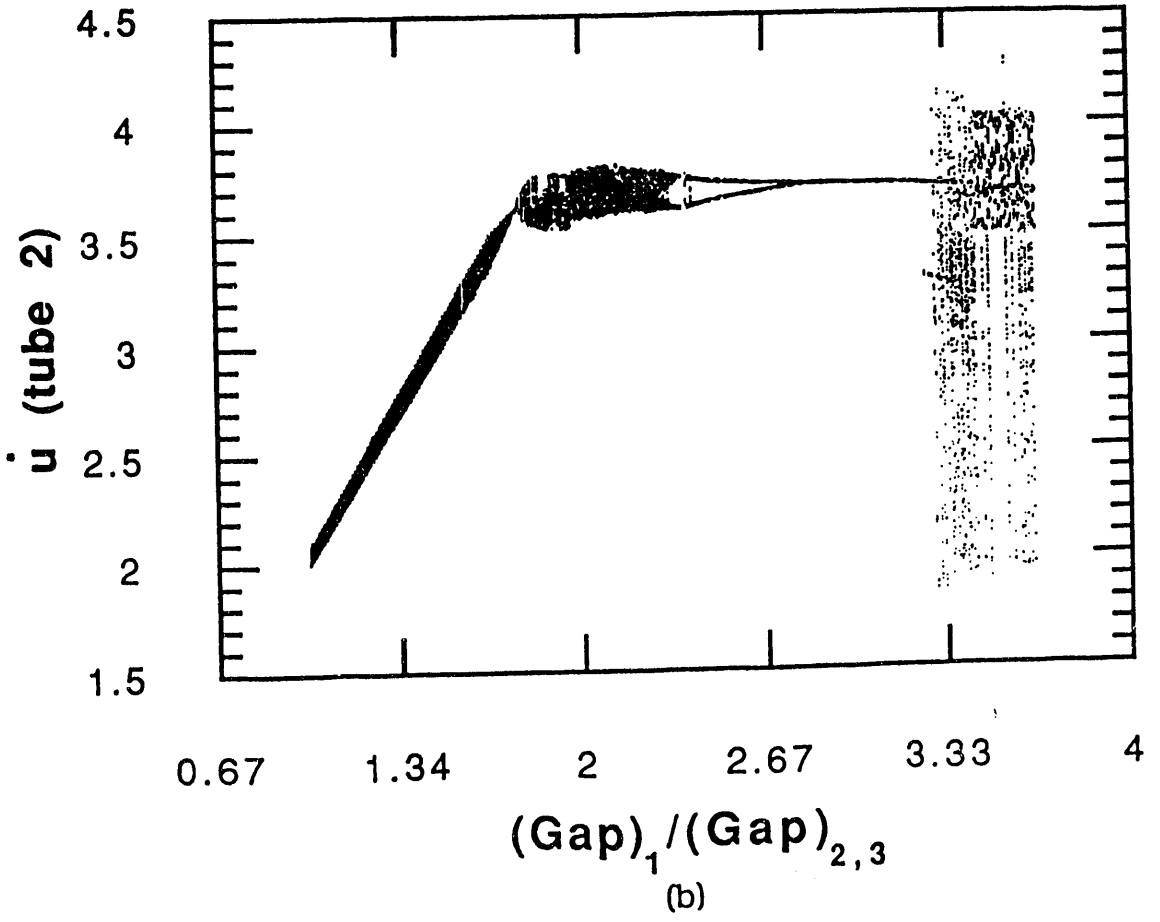

Figure 11. Bifurcation diagrams for $(gap)_1 \nleq (gap)_{2,3}$: (a) $U_v = 80$ (b) $U_v = 100$. Here, $(gap)_j$ represents the gap size of Tube j and also

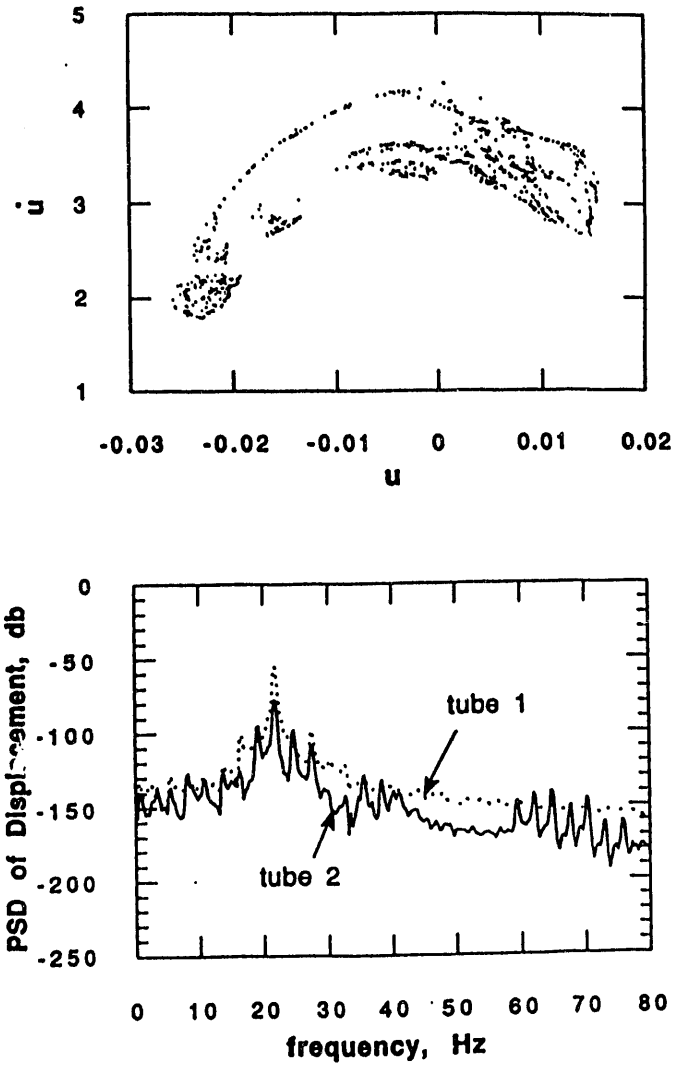

Figure 12. Poincare map & PSD for $(gap)_1 \approx (gap)_{2,3}$: $U_v = 100$, $(gap)_1/(gap)_{2,3} = 3.34$ (chaotic).

DATE
FILMED
8/23/93
END